J. Astrophys. Astr. (2018) 39:51
https://doi.org/10.1007/s12036-018-9549-y

Review

Precision pulsar timing with the ORT and the GMRT and its applications in pulsar astrophysics

BHAL CHANDRA JOSHI[1,*], PRAKASH ARUMUGASAMY[1], MANJARI BAGCHI[3,12], DEBADES BANDYOPADHYAY[4], AVISHEK BASU[1], NEELAM DHANDA BATRA[5,6], SURYARAO BETHAPUDI[7], ARPITA CHOUDHARY[3], KISHALAY DE[8], L. DEY[2], A. GOPAKUMAR[2], Y. GUPTA[1], M. A. KRISHNAKUMAR[1,9], YOGESH MAAN[10], P. K. MANOHARAN[1,9], ARUN NAIDU[11], RANA NANDI[14], DHRUV PATHAK[3,12], MAYURESH SURNIS[13,15] and ABHIMANYU SUSOBHANAN[2]

[1]National Centre for Radio Astrophysics (Tata Institute of Fundamental Research), Post Bag No 3, Ganeshkhind, Pune 411 007, India.
[2]Department of Astronomy and Astrophysics, Tata Institute of Fundamental Research, Dr. Homi Bhabha Road, Mumbai 400 005, India.
[3]The Institute of Mathematical Sciences, C. I. T. Campus, Taramani, Chennai 600 113, India.
[4]Astroparticle Physics and Cosmology Division, Saha Institute of Nuclear Physics, HBNI, 1/AF Bidhannagar, Kolkata 700 064, India.
[5]Department of Physics, Indian Institute of Technology, Hauz Khas, New Delhi 110 016, India.
[6]Department of Physics, Birla Institute of Technology and Science Pilani, Hyderabad Campus, Shameerpet Mandal, Hyderabad 500 078, India.
[7]Department of Physics, Indian Institute of Technology Hyderabad, Kandi, Hyderabad 502 285, India.
[8]Cahill Centre for Astrophysics, California Institute of Technology, 1200 East California Boulevard, Pasadena, CA 91125, USA.
[9]Radio Astronomy Centre (NCRA-TIFR), Ooty, India.
[10]ASTRON, The Netherlands Institute for Radio Astronomy, Postbus 2, 7990 AA Dwingeloo, The Netherlands.
[11]Mcgill Space Institute, McGill University, Montreal, Canada.
[12]Homi Bhabha National Institute Training School Complex, Anushakti Nagar, Mumbai 400 094, India.
[13]Department of Physics and Astronomy, West Virginia University, P. O. Box 6315, Morgantown, WV, USA.
[14]Department of Nuclear and Atomic Physics, Tata Institute of Fundamental Research, Mumbai 400 005, India.
[15]Center for Gravitational Waves and Cosmology, West Virginia University, Chestnut Ridge Research Building, Morgantown, WV, USA.
*Corresponding author. E-mail: bcj@ncra.tifr.res.in

MS received 12 July 2018; accepted 16 August 2018; published online 29 August 2018

Abstract. Radio pulsars show remarkable clock-like stability, which make them useful astronomy tools in experiments to test equation of state of neutron stars and detecting gravitational waves using pulsar timing techniques. A brief review of relevant astrophysical experiments is provided in this paper highlighting the current state-of-the-art of these experiments. A program to monitor frequently glitching pulsars with Indian radio telescopes using high cadence observations is presented, with illustrations of glitches detected in this program, including the largest ever glitch in PSR B0531+21. An Indian initiative to discover sub-μHz gravitational waves, called Indian Pulsar Timing Array (InPTA), is also described briefly, where time-of-arrival uncertainties and post-fit residuals of the order of μs are already achievable, comparable to other international pulsar timing array experiments. While timing the glitches and their recoveries are likely to provide constraints on the structure of neutron stars, InPTA will provide upper limits on sub-μHz gravitational waves apart from auxiliary pulsar science. Future directions for these experiments are outlined.

Keywords. Equation of state—gravitational waves—pulsars: general—stars: neutron.

1. Introduction

Highly magnetized rotating neutron stars, discovered first as radio pulsars emitting a train of narrow periodic pulses (Hewish *et al.* 1968), provide excellent celestial clocks, primarily due to their massive and compact nature (mass $\sim 1.4 M_\odot$; radius $\sim$10 km). A stability of their periods up to one part in 10^{20}, allows measurements in astrophysical experiments with precision, unprecedented in astronomy, for constraining Equation of State (EoS) of these stars and detecting sub-μHz gravitational waves (GW).

About 2600 pulsars have been discovered so far[1] (Manchester *et al.* 2005), which are broadly classified as normal pulsars, young pulsars and millisecond pulsars, based on their rotation period and magnetic field strength. The latter two of these classes are relevant for this paper. Young pulsars with high magnetic dipolar surface field ($10^{12} < B < 10^{14}$ G) and/or short periods ($P \sim 100$ ms) show rotational irregularities, such as abrupt spin-ups, also called glitches (Radhakrishnan & Manchester 1969; Lyne *et al.* 2000; Krawczyk *et al.* 2003; Espinoza *et al.* 2011; Yu *et al.* 2013), as well as slow wander in rotation rate, known as timing noise (Boynton *et al.* 1972; Cordes 1980; Cordes & Helfand 1980). Measurements of these rotational irregularities are useful for characterizing the internal structure of neutron star and constraining its EoS (Link *et al.* 1999, 1992; Haskell & Melatos 2015; Ho *et al.* 2015). On the other hand, older pulsars with relatively lower magnetic fields ($10^8 < B < 10^{11}$ G) and millisecond periods ($P \sim$ 1.5–30 ms) exhibit a much smaller rotational slow-down and highly stable rotation rates. An ensemble of these millisecond pulsars (MSPs) is useful as a celestial detector to measure small metric perturbation caused by GW passing near the Earth (Foster & Backer 1990; Joshi 2013). High precision observations of such ensembles are carried out by the Pulsar Timing Arrays (PTA), which are experiments for detection of sub-μHz GW (Manchester *et al.* 2013; Demorest *et al.* 2013). High-sensitivity observations using large collecting area radio telescopes, such as the Ooty Radio Telescope (ORT: Swarup *et al.* 1971) and the upgraded Giant Meterwave Radio Telescope (GMRT, uGMRT: Swarup *et al.* 1991; Gupta *et al.* 2017) are analysed with pulsar timing technique to obtain high precision measurements for such experiments.

In this paper, a brief review of state-of-the-art in this field is presented followed by a description of our efforts in this direction using the ORT and the GMRT. The plan of the paper is as follows. The pulsar timing technique is briefly described in section 2. Current constraints on neutron star structure and EoS are discussed in section 3 followed by a description of the glitch monitoring program using the ORT and the uGMRT and its preliminary results. A brief review of PTA experiments is presented in section 4 followed by details and current status of Indian PTA experiment called Indian Pulsar Timing Array (InPTA).

[1] http://www.atnf.csiro.au/people/pulsar/psrcat/.

2. Pulsar timing

Pulsar timing involves comparison of the prediction of pulse time-of-arrival (ToA) from an assumed rotational model of star with the observed ToA to refine the model parameters. The key point of this technique is keeping track of rotation cycles of pulsar, which improves precision as a function of time. As discussed below, the assumed model is usually complex involving several parameters, all of which are estimated in this process.

As pulsars are weak sources, ToAs are measured from an average pulse, obtained after averaging the pulsed time series over several thousand pulses. A fiducial point on the pulse is chosen, which usually comes with a random shift from a noise-free template in a given observation. Template matching is used to find this shift and adjust time of observations (Taylor 1992) to get the ToA of the pulse up to a precision of few nano-seconds using an atomic clock, usually a hydrogen maser synchronized to an international time scale, called Temps Atomic Internationale.

These observed ToAs are first referred to Solar System Barycentre (SSB – an inertial frame) and then onwards to an inertial frame for the pulsar as shown below:

$$t_{\rm p} = t_{\rm topo} + t_{\rm clock} - D/f^2 + \Delta_{\rm R} + \Delta_{\rm S} + \Delta_{\rm E}, \qquad (1)$$

where $t_{\rm topo}$ are observed topocentric ToAs, $t_{\rm clock}$ are clock corrections, D is the dispersion constant accounting for dispersive delay in the inter-stellar medium and $\Delta_{\rm R}$, $\Delta_{\rm S}$ and $\Delta_{\rm E}$ are the Roemer, Shapiro and Einstein delays respectively (see Stairs (2003) for details on these delays). Additionally, the timing model may also include dynamics of the star itself and that of its companion if the pulsar happens to be in a binary system. Finally, the timing model also assumes a rotational model of the neutron star given by

$$\nu(t) = \nu_0 + \dot{\nu}(t - t_0) + \frac{1}{2}\ddot{\nu}(t - t_0)^2, \qquad (2)$$

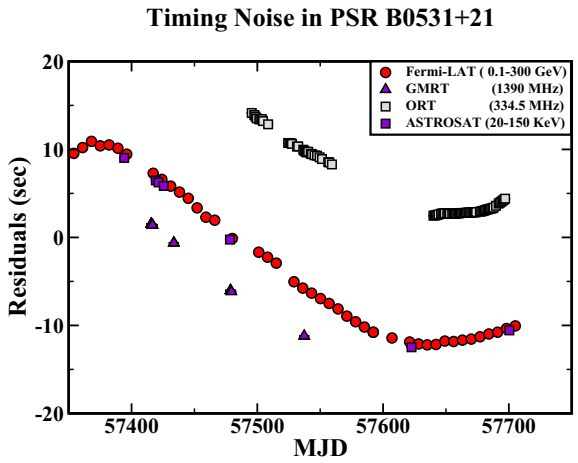

Figure 1. Timing noise seen in the rotation rate of Crab pulsar (PSR B0531+21) from radio- to high-energies. The data are from the ORT, the legacy GMRT and the ASTROSAT. We also used archival data obtained by Fermi telescope. The timing noise, which is a slow wander of rotation rate, is seen as systematic deviation from zero residuals. The timing residuals for the four telescopes are offset from each other by the amount of relative offset in the data acquisition pipeline

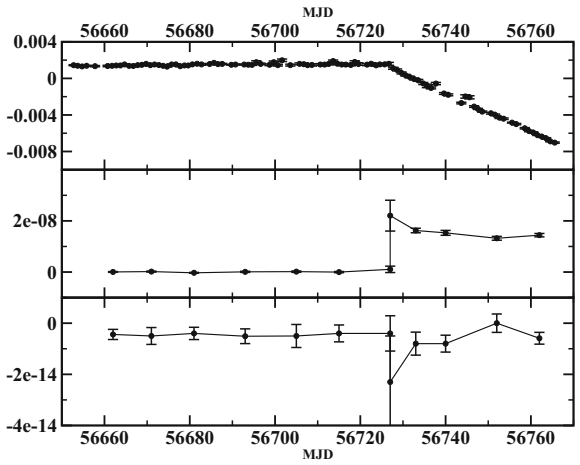

Figure 2. A small glitch detected in PSR B0740−28 at the ORT on MJD 56727. The top panel shows the pre- and post-glitch timing residuals as a function of MJD. The middle panel shows pre- and post-glitch spin frequency (ν) and the bottom panel shows the frequency derivative ($\dot{\nu}$). The pulsar was observed at 334.5 MHz.

where ν, ν_0, $\dot{\nu}$ and $\ddot{\nu}$ are the rotational frequency and its higher order derivatives assumed at an epoch t_0. The timing model is used to predict the pulse number N,

$$N = \nu(t - t_0). \tag{3}$$

If the prediction is correct, N should be an integer. If not, the fractional part, called timing residual, is minimized in a least-square sense to obtain the best-fit parameters of the model (see Edwards *et al.* (2006) for more details).

The timing model is usually complex. The commonly included parameters are pulsar spin period and its higher-order derivatives, position and proper motion of the star, parallax, dispersion measure[2] (DM) and binary Keplerian and post-Keplerian parameters, such as orbital period, orbital separation, component masses, advance of periastron, orbital period decay, gravitational red-shift and range and shape of Shapiro delay in the binary. In addition, model of the solar wind, ephemeris for solar system bodies and position of the Sun in the absolute International Celestial Reference Frame also play a role.

A 'good model' yields 'white noise' timing residuals, whereas systematics in timing residuals imply unmodeled effects. One such unmodeled effect is timing noise. An example is shown in Fig. 1 for PSR B0531+21 from our high cadence monitoring of this pulsar with the ORT and the GMRT. Another rotational irregularity is pulsar glitch, seen as an abrupt increase in rotation rate of the star, illustrated in Fig. 2 for PSR B0740−28. Also relevant to this paper is systematics in the timing residuals of an ensemble of pulsars due to correlated unmodeled perturbation caused by a passing GW. A precision of tens of nanoseconds is already achieved in experiments to detect GW.

3. Monitoring pulsar glitches

3.1 *Pulsar glitches and the internal structure of neutron stars*

Glitches provide a peek into the internal structure of the neutron star. Initially, glitches were interpreted as star-quakes (Pines & Shaham 1972). Now, glitches are believed to be the result of transfer of angular momentum from a differentially rotating interior super-fluid to the star-crust (Anderson & Itoh 1975). Direct evidence of such super-fluid is inferred from the cooling rate of neutron star in CasA (Baym *et al.* 1971; Heinke & Ho 2010; Shternin *et al.* 2011). It is energetically more favourable for vortex cores of super-fluid to 'pin' at lattice sites in the crust, magnetically or otherwise (Alpar 1977; Link 2009, 2012a, b). This leads to conservation of areal density of super-fluid vortex constraining the super-fluid rotation to be a constant. While crust slows down due to electromagnetic torques, associated 'pinned' neutron super-fluid component cannot

[2]Dispersion Measure is the integrated column density of electrons in the line-of-sight.

slow down and develops a differential rotation storing angular momentum. When the differential rotation between the crust and 'pinned' super-fluid exceeds a critical lag, the magnus force is large enough to 'unpin' crustal super-fluid and the stored angular momentum is transferred from the super-fluid to the crust during a glitch event (Link *et al.* 1999).

Till date, 529 glitches have been reported in 188 pulsars (Espinoza *et al.* 2011) with about 36 pulsars having 4 or more glitches.[3] Most glitching pulsars are young with characteristic ages of about 100 kyr. There are two broad types of glitches: Crab-like (Crab pulsar – PSR B0531+21 with 27 reported glitches), which are small amplitude glitches and are accompanied by a permanent change in spin-down, and vela-like (Vela pulsar – B0833−45 with 20 reported glitches), which are very regular large amplitude glitches with linear recovery (Espinoza *et al.* 2011). There are pulsars, which show both large and small glitches, such as PSRs B1046−58, B1338−62 and B1737−30. This bimodality is apparent from a distribution of fractional glitch sizes shown in Fig. 3. While the reasons for this dichotomy are unknown, one possibility is that small and large glitches originate in different parts of the star, with neutron star crust contributing to smaller glitches, whereas the core participates in larger glitches. Thus, glitches can provide a probe of structure as well as EoS of the star.

An important sub-class of glitching pulsars is pulsars with frequent glitches. PSRs J0537−6910 (23 glitches), B1338−62 (23 glitches) and B1737−30 (35 glitches) are the best known representatives of this class. The frequent glitches in these pulsars show almost a linear cumulative spin-up, when averaged over all the glitches in a pulsar. The average rate of angular momentum transferred can be estimated from observed cumulative spin-up of the crust. Equating this to average rate of angular momentum transferred from the reservoir ($I_{\rm res}\,\dot{\nu}$), a lower limit on crustal super-fluid ($I_{\rm res}/I_{\rm c}$) can be obtained from observations and implies that about 0.9 to 1.8% of Moment of Inertia (MoI) of the star participates in these glitches (Link *et al.* 1999).

It is possible to theoretically estimate crustal MoI assuming a given EoS. A comparison with the observed glitch sizes would be interesting to examine if all glitches originate in the crust. Such a comparison can become even more constraining if one considers non-dissipative coupling of inter-penetrating neutron super-fluid and $e-p$ normal fluid, called 'entrainment' (Chamel & Carter 2006; Chamel 2013). It has been shown in laboratory experiments that the net effect of

[3] http://www.jb.man.ac.uk/pulsar/glitches/gTable.html.

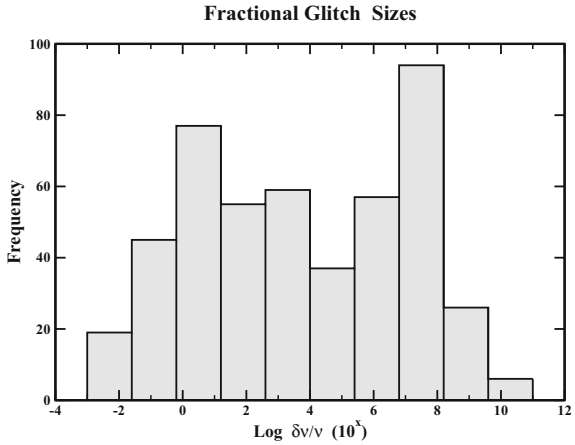

Figure 3. The bi-modal distribution of fractional glitch sizes of all the reported pulsar glitches.

entrainment is an increase in the effective neutron mass by a factor of about 4.3−5.1 (Andersson *et al.* 2012; Delsate *et al.* 2016). This increases the lower limit for MoI of reservoir to about 7% for Vela pulsar and brings EoS in tension with data as the crustal super-fluid is just not enough (Andersson *et al.* 2012) to explain the glitch events. Possible solutions being explored range from large glitching pulsars being low mass neutron star ($<1.1M$), core super-fluid also acting as a reservoir, or lack of precision in theory (ill-defined crust-core boundary, Piekarewicz *et al.* 2014). Both observational and theoretical work is required.

Lastly, coupling between different components of neutron star can be probed by post-glitch relaxation, characterized by an exponential or linear recovery or both, often with single or multiple components (Yu *et al.* 2013). Often, monitoring pulsar observations are carried out once a month and we miss out details of such recoveries. A high cadence campaign triggered by the glitch event are needed to investigate the recoveries more effectively.

3.2 *Monitoring pulsar glitches with the ORT and the uGMRT*

We have recently started a program for high cadence monitoring of pulsar glitches using the ORT and the uGMRT. The ORT observations are carried out once every three days for a sample of 11 most frequently glitching pulsars (with a glitch rate of about one per year) at 334.5 MHz. A real-time automated pipeline for detecting glitches soon after the observations is being developed and implemented at the ORT (Basu and Joshi, in preparation), which will allow triggering daily observations as soon as a glitch is detected. This is likely to allow studying recoveries in greater details. Likewise,

uGMRT is being used to monitor 11 frequently glitching pulsars at Band 4 (550–950 MHz) and Band 5 (1100–1400 MHz) with the uGMRT (see details of frequency bands in Gupta *et al.* (2017)).

In this program, we have detected 5 glitches so far. Figure 2 shows a glitch event with a fractional glitch amplitude of $3.5 \pm 1 \times 10^{-9}$ and recovery time constant of about five days. The estimated glitch epoch is MJD 56727 with an error of about half a day. This was the first glitch we detected and the short recovery motivated the higher cadence program that we are currently running. In November 2017, we detected the largest ever glitch in the Crab pulsar, which is shown in Fig. 4 (Krishnakumar *et al.* 2017). Two glitches in Vela pulsar (PSR B0833−45) were also detected in September 2014 (Fig. 5) and December 2016 with fractional glitch amplitudes of 3.8×10^{-7} and 7.8×10^{-8} respectively. While these examples illustrate the potential of our program even without an automated glitch pipeline,

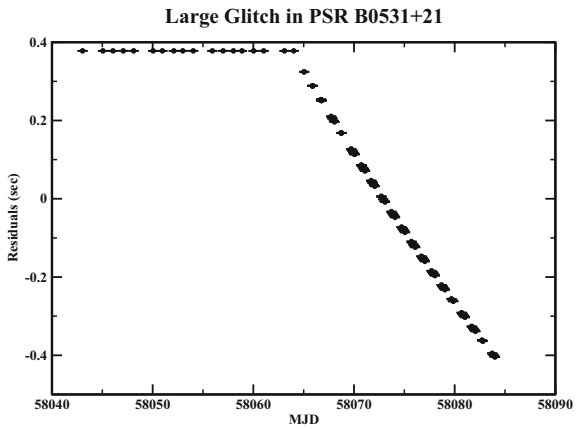

Figure 4. The largest ever detected glitch in Crab pulsar (PSR B0531+21) on MJD 58064 observed with the ORT.

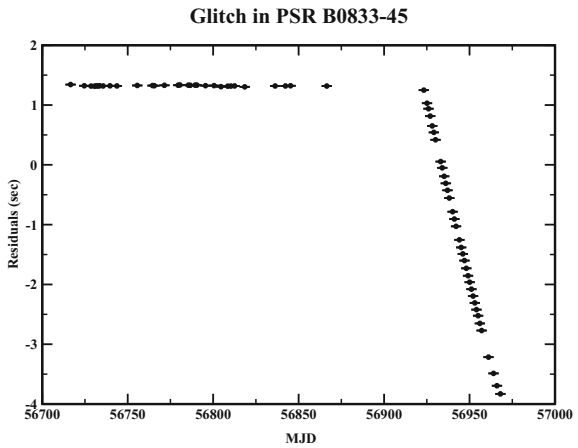

Figure 5. A glitch observed in Vela pulsar (PSR B0833−45) on MJD 56922 observed with the ORT.

the pipeline will provide measurements of recoveries in a larger sample of pulsars constraining the coupling between different components of the neutron star.

In addition, theoretical work is under way to estimate the fractional MoI of the crust using a unified relativistic mean field approach towards developing a single EoS of crust and core. This can then be compared with estimates of fractional MoI of the super-fluid responsible for the glitches to check if this super-fluid is entirely crustal or a participation of core is also needed (Basu *et al.* 2018a).

4. Pulsar timing arrays

GW were unique distinguishing feature of general theory of relativity, when it was proposed by Einstein (Einstein 1918). The indirect indication in the first double neutron star system (Hulse & Taylor 1975; Weisberg *et al.* 2010) has now been confirmed by direct detection by aLIGO (Abbott *et al.* 2016, 2017 and references therein).

A wide variety of binaries with compact objects, such as white dwarf − white dwarf binaries, neutron star – white dwarf binaries, neutron star – neutron star binaries (double pulsar, GW170817), neutron star – black hole binaries, black hole – black hole (GW150914, GW151226, GW170104, GW170814, GW170608) and super-massive black hole binary systems (SMBHB), form the sources of GWs, with their spectrum ranging from 300 pHz to 100 kHz (Joshi 2013). While aLIGO and LISA are sensitive at higher frequency range (10 Hz to 100 KHz for aLIGO and 0.1 Hz to few μHz for LISA), the sources of relevance for PTA are SMBHB systems, emitting GWs in sub-μHz frequencies. These reside in the centers of galaxies. One good example is SMBHB OJ287 (Sillanpää *et al.* 1988; Valtonen *et al.* 2010, 2011a, b, 2012, 2016) with two super-massive black holes of masses 18 billion and 150 million solar masses and an orbital period of twelve years. A random superposition of GWs from several such sources in all directions of sky forms a stochastic gravitational wave background (SGWB). The main goal of a PTA is to detect this background. Taking into account various evolutionary scenarios, Jaffe and Backer (2003) proposed the following spectrum of SGWB:

$$h_c(f) = 10^{-15} \left(\frac{f}{\mathrm{yr}^{-1}} \right)^{-2/3}, \tag{4}$$

where h_c is the dimensionless characteristic strain.

This spectrum is easiest to detect with a PTA. Thus, PTA, essentially a large celestial instrument constructed

using an ensemble of pulsars, cover a frequency range complimentary to other GW experiments.

A passing GW causes a perturbation in space-time fabric, which is imprinted as a tiny fluctuation in ToA measurements of pulsars. Analysis of this systematic effect using pulsar timing could be used to detect these waves (Sazhin 1978; Detweiler 1979; Hellings & Downs 1983; Foster & Backer 1990). The first PTA experiment started in 2003 with Parkes Radio Telescope and currently four experiments are operational sharing their data in an international collaboration called International Pulsar Timing Array (IPTA).

4.1 *Pulsars as GW telescope*

The effect of propagating perturbations in space-time metric is to advance or retard the time of a pulsar's electromagnetic pulse, which serves as a time marker. This results in a fractional frequency change, $\frac{\delta\nu}{\nu}$, given by

$$\frac{\delta\nu}{\nu} = \frac{1}{2}\cos 2\psi(1-\cos\theta)(h_{\rm e}(t) - h_{\rm p}(t-d/c-d\cos\theta/c)). \quad (5)$$

Here, the Earth, assumed to be at the origin of the co-ordinate system, encounters a GW propagating in the z direction with its polarization making an angle ψ with the x-axis. The line-of-sight to the pulsar in the x–z plane makes an angle θ with the direction of the GW propagation. The effect of GW passing near the Earth and near the pulsar are represented by dimensionless strains $h_{\rm e}$ and $h_{\rm p}$ respectively. These terms are also called 'earth' and 'emission/pulsar' terms. While the 'pulsar' term in general will be uncorrelated from pulsar to pulsar, the 'earth' term will be correlated over a pair of pulsars due to the presence of GWs. This correlation over an ensemble of pulsars represents 'antenna pattern' of a PTA and is excited completely due to isotropic nature of SGWB (Hellings & Downs 1983). PTA experiment uses this correlation to detect or to set an upper limit on SGWB.

A good PTA requires (a) pulsars with exceptionally high rotational stability, (b) a sample of pulsars more or less uniformly distributed in the sky, (c) pulsars with high signal-to-noise ratio pulse detections, (d) pulsars with stable pulse shapes, and (d) pulsars on line-of-sights without complicated propagation effects. Thus, while 2600 pulsars are known today, only about 60 satisfy these requirements. Even this ensemble does not provide a uniform coverage, which is a real limitation for searches of GWs from isolated SMBHB and a search for GW burst memory (see section 4.2). Moreover, DM variations have a long time-scale, which introduces a red-noise in ToAs very similar to a GW signal and require simultaneous high cadence multi-frequency observations. However, it is not clear if this systematic can entirely be removed (Cordes *et al.* 2016). The non-uniform distribution of pulsars in the sky can along-with DM variations produce an artifact GW signal. The ORT and the uGMRT can help in finding new 'good clocks' with large scale pulsar surveys and simultaneous high cadence multi-frequency observations.

4.2 *GW sources for PTA*

PTAs are sensitive to GWs radiated by mainly three types of sources: (1) isotropic SGWB, (2) GWs from individual SMBHB and gravitational burst sources with memory. As discussed earlier, SGWB is formed by a random superposition of GWs from an ensemble of SMBHB systems. SMBHB are formed during the merger of two galaxies, which have seed black hole at their centers. A simple model of the post merger evolution suggests a spectrum given in equation (4). However, recent work shows that the amplitude and shape of this spectrum depends on hierarchical assembly models of SMBHB systems (Sesana *et al.* 2008). This study computed the GW spectrum in the frequency range of PTAs and concluded that the expected SGWB signal could be lower by a factor of three than the current PTA limits. Further, mechanisms have been proposed, which imply a complete stalling of significant evolution of binary orbits (see Dvorkin & Barausse 2017). In addition, factors, such as eccentricity in SMBHB, a stronger interaction with environment as well as lack of precision in scaling relations (Sesana *et al.* 2016), also diminish the strain spectrum well below that predicted in Sesana *et al.* (2008). While alternative mechanisms have been proposed, their impact is yet to be evaluated. These scenarios make a PTA detection of SGWB challenging and the tension between PTA limits and expected SGWB is already probing formation and evolution mechanism of SMBHB system.

Can PTA detect individual SMBHB? Sesana *et al.* (2009) carried out Monte Carlo simulations with twelve different models involving different scaling relations to show that all models predict at least one resolved SMBHB which is detectable for timing residuals in the range of 5–50 ns.

Lastly, PTAs are sensitive to GW bursts with memory. GW memory has been known for last four decades (Zel'dovich & Polnarev 1974; Braginskii & Grishchuk 1985; Braginskii & Thorne 1987) in its linear form for flyby interactions, but was shown to exist for

bound systems such as coalescing binaries by Blanchet & Damour (1992) and Thorne (1992). GW memory is a phenomenon where passing GW leaves a permanent deformation in space-time. With two to three weeks of observational cadence and significant growth in timing residuals due to GW memory over a day, the change in metric due to GW memory appears like a jump in timing residuals similar to pulsar glitch. Unlike a pulsar glitch, which is seen in a single pulsar, a GW burst is likely to produce correlated jumps in TOAs of at least those pulsars, which are sensitive in the PTA antenna pattern towards the direction of GW burst. GW burst with memory are unlikely to be detected in aLIGO, but are expected to be stronger for LISA and PTA bands (Favata 2010).

4.3 *Current status of PTA experiments*

The longest running experiment is Parkes Pulsar Timing Array (PPTA), which started in 2003 (Manchester *et al.* 2013). It uses Parkes radio telescope between 730 to 1400 MHz to monitor a sample of 25 MSPs, once every three weeks (Manchester *et al.* 2013). The second experiment is North American Nano-hertz Observatory for gravitational waves (NANOgrav), which uses GBT and Arecibo telescope to monitor 45 pulsars every 20−30 days since 2005 (Arzoumanian *et al.* 2018). In the last few years, seven major European telescopes have combined to form European Pulsar Timing Array (EPTA: Desvignes *et al.* 2016). An Indian experiment is described later in this article.

Since PTAs were first proposed, there has been three orders of magnitude improvement in sensitivity in the last 25 years. The current best limits on SGWB are 1.5×10^{-15} from NANOgrav collaboration (Arzoumanian *et al.* 2018). All PTAs pool their data as IPTA data release. This is useful as it (a) allows cross comparison and calibration of different PTAs, and (b) increases the number of pulsars and cadence of observations, thus improving the sensitivity of PTAs collectively. A data combination from all PTAs as IPTA data release puts the limit at 1.7×10^{-15} (Verbiest *et al.* 2016), which is likely to improve by a factor of two with improved alternative data combination schemes.

As no SGWB is detected up to a limit on GW strain amplitude of 10^{-15}, contrary to expectations, this calls calculations based on previous models in question (see section 4.2). In addition, recent work points to lack of precision in known solar system ephemeris, which define the location of SSB, critical for precision in pulsar timing (Lazio *et al.* 2018). Indeed, lack of detection of GWs can be used to rule out the so-called unidentified massive objects (UMOs) in the solar system (Guo *et al.* 2018). Apart from non-detection of SGWB, any individual source has also not been detected so far up to a limit of 0.6×10^{-14} (Babak *et al.* 2016). Finally, PTA experiments constrain the rate at which we encounter bursts with memory, with amplitudes greater than 10^{-13}, to less than 1.5 yr^{-1} (Arzoumanian *et al.* 2015).

4.4 *Indian Pulsar Timing Array (InPTA)*

In 2015, an Indian experiment using Tata Institute of Fundamental Research's two facilities, the ORT and the GMRT, was initiated as a pilot project (Joshi *et al.* 2015). This experiment has been operating for three years and is called Indian Pulsar Timing Array (InPTA). This is a collaborative experiment involving five institutions in India and about 18 researchers[4] and students. Initially, we used a sample of nine carefully chosen MSP, which were observed once every 20 days with the GMRT at a frequency of 1.4 GHz. The main difference in our experiment from other PTAs is a very high 'cadence' or frequency of observations at 334 MHz using the ORT. Unlike other PTAs, we also carried out simultaneous coordinated observations with the two telescopes with a view to obtain more accurate characterization of epoch-to-epoch DM variation.

The GMRT has been recently upgraded with wide-band feeds at Band 3 (250–500 MHz), Band 4 (550–850 MHz) and Band 5 (1060–1460 MHz) and a new digital backend, which provides four simultaneous beams in the sky with real-time coherent de-dispersion capability in two beams (Gupta *et al.* 2017; Reddy *et al.* 2017). This upgraded GMRT (uGMRT) promises to be a powerful instrument for precision pulsar timing. We started a pilot project to characterize the timing precision of uGMRT in 2016 (Gupta *et al.* 2016). In this experiment, we also selected additional PTA pulsars. While a single band was used in the experiment initially, gradually two additional bands were added for simultaneous observations as the uGMRT upgrade progressed over the last two years with coherent de-dispersion capability included in the past year. After gaining confidence with new upgraded system, this experiment is now merged with InPTA to form a single experiment.

The current InPTA monitors a sample of 20 PTA pulsars once every 14 days with the three bands (Bands 3, 4 and 5) simultaneously using the uGMRT. In addition,

[4] B. C. Joshi, A. Gopakumar, M. Bagchi, Y. Gupta, A. Choudhary, Arun Naidu, S. Abhimanyu, D. Pathak, M. A. Krishnakumar, P. K. Manoharan, M. Surnis, N. Dhanda Batra, P. Arumugasamy, K. Dey, S. Desai, S. Bethapudi, Y. Maan and L. Dey.

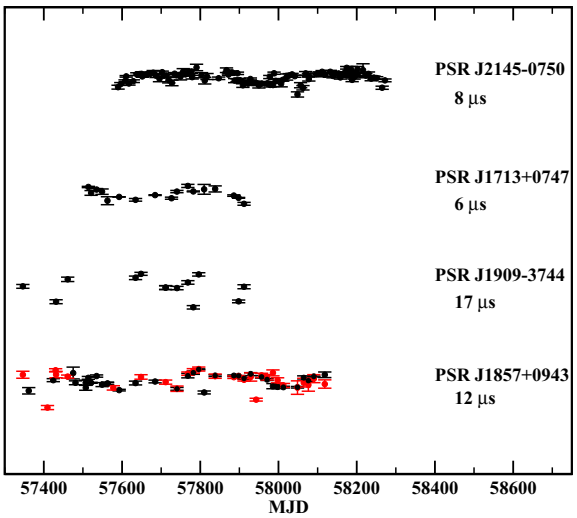

Figure 6. The timing residuals after fitting timing solutions for a sample of pulsars observed as part of InPTA.

eleven of these pulsars are observed once every three days with the ORT at 334.4 MHz for high cadence monitoring of DM variations. While Band 5 observations with the uGMRT provide high precision ToAs for GW analysis, Band 3 and Band 4 observations with uGMRT and ORT are used for correcting DM variations. Each pulsar is observed for duration ranging from 30 to 45 min.

The first year of our project was used to improve observatory clocks and to find the relative offsets between our two telescopes. The offsets, which introduce systematics in the estimate of dispersion delay in ToA at two different frequencies, were measured by radiating an artificial pulsar like signal and by analysing simultaneous observations of PSR B0531+21 with the ORT, the GMRT, the ASTROSAT and Fermi in a campaign for another experiment (Fig. 1, see also Basu *et al.* 2018b).

With these improvements, we have routinely been getting ToAs with uncertainties ranging from 1 to 30 μs for most pulsars in our sample. Although the signal-to-noise ratio varies from epoch to epoch, we typically get 40 to 200 signal-to-noise ratio profiles. Currently, work is in progress to better reject radio frequency interference and take into account diffractive inter-stellar scintillation.

We have obtained phase connected solutions[5] for our pulsars by making use of the higher cadence ORT observations. The multi-frequency observations were then used to estimate epoch-to-epoch variations of DM, which were compensated to obtain post-fit timing residuals for each pulsars. As an illustration, Fig. 6 shows the best-fit residuals of four pulsars in our sample. The typical post-fit residuals obtained by us range from 8 to 17 μs. While these are comparable to other PTAs in the world, we are refining our timing solutions to achieve sub-μs residuals. These will be eventually used in GW analysis to obtain InPTA limits and such an analysis is in progress.

[5]Phase connected solution refers to a timing model, which accounts for every pulsar rotation without phase ambiguities.

5. Summary and future prospects

We are operating a glitch detection program at the uGMRT and the ORT with high cadence monitoring of a sample of frequently glitching pulsars. We have detected 5 glitches so far, including the largest ever Crab pulsar glitch. These observations are likely to provide constraints on MoI of crustal super-fluid and to probe coupling of the pinned super-fluid to the rest of the star. An Indian initiative to discover sub-μHz GW called InPTA is under way using the ORT and the uGMRT. ToA uncertainties of the order of μs are already achievable, comparable to other international PTA experiments. Post-fit residuals of the order of μs have been achieved and work is in progress to evaluate upper limits on GWs from these observations.

Efforts are on to increase the ensemble of PTA pulsars with companion pulsar surveys with uGMRT to find more good clocks with 'good white noise' characteristics. InPTA is striving to improve interoperability with IPTA and share data, while carrying out GW analysis for search of GWs from SGWB, individual GW sources, and GW burst with memory.

Lastly, a future dedicated PTA experiment is being explored using currently out of use two 30-m communication antennas owned by a private telecommunication company. A phased array of these antennas, located near GMRT, is being proposed by us as Tata Pulsar Timing Array, for daily observations of PTA pulsars with ultra-wideband receivers. Such high cadence monitoring is likely to significantly improve sensitivity of PTAs (Siemens *et al.* 2013).

Acknowledgements

The authors acknowledge help and support provided by the staff at Radio Astronomy Centre, Ooty and Giant Meterwave Radio Telescope during these observations. The ORT and the GMRT are operated by the National Centre for Radio Astrophysics. BCJ, MAK

and PKM acknowledge support from DST-SERB Grant EMR/2015/000515. YM acknowledges use of the ERC funding from the (FP/2007-2013)/ERC Grant Agreement No. 617199.

References

Abbott B. P., Abbott R., Abbott T. D. *et al.* 2016, Phys. Rev. Lett. 116, 061102

Abbott B. P., Abbott R., Abbott T. D. *et al.* 2017, ApJ, 851, L35

Alpar M. A. 1977, ApJ, 213, 527

Anderson P. W., Itoh N. 1975, Nature, 256, 25

Andersson N., Glampedakis K., Ho W. C. G., Espinoza C. M. 2012, Phys. Rev. Lett., 109, 241103

Arzoumanian Z., Brazier A., Burke-Spolaor S. *et al.* 2015, ApJ, 810, 150

Arzoumanian Z., Baker P. T., Brazier A. *et al.* 2018, ApJ, 859, 47

Babak S., Petiteau A., Sesana A. *et al.* 2016, MNRAS, 455, 1665

Basu A., Char P., Nandi R., Joshi B. C., Bandyopadhyay D. 2018a, ArXiv e-prints, arXiv:1806.01521

Basu A., Joshi B. C., Bhattacharya D. *et al.* 2018b, arXiv e-prints, arXiv:1806.01066

Baym G., Bethe H. A., Pethick C. J. 1971, Nucl. Phys. A, 175, 225

Blanchet L., Damour T. 1992, Phys. Rev. D, 46, 4304

Boynton P. E., Groth E. J., Hutchinson D. P. *et al.* 1972, ApJ, 175, 217

Braginskii V. B., Grishchuk L. P. 1985, Zhurnal Eksperimentalnoi i Teoreticheskoi Fiziki, 89, 744

Braginskii V. B., Thorne K. S. 1987, Nature, 327, 123

Chamel N. 2013, Phys. Rev. Lett., 110, 011101

Chamel N., Carter B. 2006, MNRAS, 368, 796

Cordes J. M. 1980, ApJ, 237, 216

Cordes J. M., Helfand D. J. 1980, ApJ, 239, 640

Cordes J. M., Shannon R. M., Stinebring D. R. 2016, ApJ, 817, 16

Delsate T., Chamel N., Gurlebeck N. *et al.* 2016, Phys. Rev. D, 94, 023008

Demorest P. B., Ferdman R. D., Gonzalez M. E. *et al.* 2013, ApJ, 762, 94

Desvignes G., Caballero R. N., Lentati L. *et al.* 2016, MNRAS, 458, 3341

Detweiler S. 1979, ApJ, 234, 1100

Dvorkin I., Barausse E. 2017, MNRAS, 470, 4547

Edwards R. T., Hobbs G. B., Manchester R. N. 2006, MNRAS, 372, 1549

Einstein A. 1918, Sitzungsberichte der Koniglich Preuischen Akademie der Wissenschaften (Berlin), Seite 154–167

Espinoza C. M., Lyne A. G., Stappers B. W., Kramer, M. 2011, MNRAS, 414, 1679

Favata M. 2010, Class. Quantum Gravit., 27, 084036

Foster R. S., Backer, D. C. 1990, ApJ, 361, 300

Guo Y. J., Lee K. J., Caballero R. N. 2018, MNRAS, 475, 3644

Gupta Y., Joshi B. C., Gopakumar A. *et al.* 2016, GMRT Obs. Propos., 30-043, 1

Gupta Y., Ajithkumar B., Kale H. S. *et al.* 2017, Curr. Sci., 113, 707

Haskell B., Melatos A. 2015, Int. J. Mod. Phys. D, 24, 1530008

Heinke C. O., Ho W. C. G. 2010, ApJL, 719, L167

Hellings R. W., Downs G. S. 1983, ApJ, 265, L39

Hewish A., Bell S. J., Pilkington J. D. H., Scott P. F., Collins R. A. 1968, Nature, 217, 709

Ho W. C. G., Espinoza C. M., Antonopoulou D., Andersson N. 2015, Sci. Adv., 1, e1500578

Hulse R. A., Taylor J. H. 1975, ApJ, 195, L51

Jaffe A. H., Backer, D. C. 2003, ApJ, 583, 616

Joshi B. C. 2013, Int. J. Mod. Phys. D, 22, 1341008

Joshi B. C., Gopakumar A., Bagchi M. *et al.* 2015, GMRT Obs. Propos., 29-064, 1

Krawczyk A., Lyne A. G., Gil J. A., Joshi B. C. 2003, MNRAS, 340, 1087

Krishnakumar M. A., Joshi B. C., Basu A., Manoharan P. K. 2017, The Astronomers Telegram, 10947

Lazio T. J. W., Bhaskaran S., Cutler C. *et al.* 2018, ArXiv e-prints, arXiv:1801.02898

Link B. 2009, Phys. Rev. Lett., 102, 131101

Link B. 2012a, MNRAS, 421, 2682

Link B. 2012b, MNRAS, 422, 1640

Link B., Epstein R. I., Lattimer J. M. 1999, Phys. Rev. Lett., 83, 3362

Link B., Epstein R. I., van Riper K. A. 1992, Nature, 359, 616

Lyne A. G., Shemar S. L., Graham-Smith F. 2000, MNRAS, 315, 534

Manchester R. N., Hobbs G. B., Teoh A., Hobbs M. 2005, AJ, 129, 1993

Manchester R. N., Hobbs G., Bailes M. *et al.* 2013, Proc. Astr. Soc. Aust., 30, 17

Piekarewicz J., Fattoyev F. J., Horowitz C. J. 2014, Phys. Rev. C, 90, 015803

Pines D., Shaham J. 1972, Phys. Earth Planet. Inter., 6, 103

Radhakrishnan V., Manchester R. N. 1969, Nature, 222, 228

Reddy S. H., Kudale S., Gokhale U. *et al.* 2017, J. Astronom. Instrum., 6, 1641011

Sazhin M. V. 1978, Sov. Astron., 22, 36

Sesana A., Shankar F., Bernardi M., Sheth R. K. 2016, MNRAS, 463, L6

Sesana A., Vecchio A., Colacino C. N. 2008, MNRAS, 390, 192

Sesana A., Vecchio A., Volonteri M. 2009, MNRAS, 394, 2255

Shternin P. S., Yakovlev D. G., Heinke C. O., Ho W. C. G., Patnaude D. J. 2011, MNRAS, 412, L108

Siemens X., Ellis J., Jenet F., Romano J. D. 2013, Class. Quantum Gravit., 30, 224015
Sillanpää A., Haarala S., Valtonen M. J., Sundelius B., Byrd G. G. 1988, ApJ, 325, 628
Stairs I. H. 2003, 5, URL (cited on 2008/02/16). http://relativity.livingreviews.org/Articles/lrr-2003-5
Swarup G., Ananthakrishnan S., Kapahi V. K. *et al.* 1991, Curr. Sci., 60, 95
Swarup G., Sarma N. V. G., Joshi M. N. *et al.* 1971, Nat. Phys. Sci., 230, 185
Taylor J. H. 1992, Philos. Trans. R. Soc. A, 341, 117
Thorne K. S. 1992, Phys. Rev. D, 45, 520
Valtonen M. J., Ciprini S., Lehto H. J. 2012, MNRAS, 427, 77
Valtonen M. J., Lehto H. J., Takalo L. O., Sillanpää A. 2011a, ApJ, 729, 33
Valtonen M. J., Mikkola S., Lehto H. J. *et al.* 2011b, ApJ, 742, 22
Valtonen M. J., Mikkola S., Merritt D. *et al.* 2010, ApJ, 709, 725
Valtonen M. J., Zola S., Ciprini S. *et al.* 2016, ApJL, 819, L37
Verbiest J. P. W., Lentati L., Hobbs G. *et al.* 2016, MNRAS, 458, 1267
Weisberg J. M., Nice D. J., Taylor J. H. 2010, ApJ, 722, 1030
Yu M., Manchester R. N., Hobbs G. *et al.* 2013, MNRAS, 429, 688
Zel'dovich Y. B., Polnarev A. G. 1974, Soviet Astron., 18, 17